Global Journal of Researches in Engineering: G
Industrial Engineering
Volume 17 Issue 1 Version1.0 Year 2017
Type: Double Blind Peer Reviewed International Research Journal
Publisher: Global Journals Inc. (USA)
Online ISSN: 2249-4596 & Print ISSN: 0975-5861

A Theoretical Study of the Influence of the Injection Velocity on the Heat and Fluid Flow in A Soaking-Pit Furnace when using Flameless Oxyfuel Heating

By Mersedeh Ghadamgahi, Patrik Ound, Nils.A.I Andresson & Par Jonsson
KTH Royal Institute of Technology

Abstract- Flameless oxyfuel combustion is one of the most recently developed combustion systems that has the potential to provide better combustion efficiency combined with a lower pollution production compared to conventional combustion systems. However, a lack of knowledge exists with respect to the influence of different parameters on the combustion results when using the flameless oxyfuel technology. Thus, in the current study a previously validated CFD model is used to investigate the effect of the injection velocity on the temperature distribution, recirculation ratio of the flue gases, flame volume, turbulence intensity, and flame radiation to the ingots. The results show that an increased injection velocity highly affects the temperature uniformity inside the chamber. More specifically, the maximum temperature difference in the flame region drops from 8.59% to 3.78% for burner capacities of 130 kW and 907 kW, respectively.

Keywords: *soaking PIT furnace, CFD, oxy-fuel combustion, flame, heat transfer.*

GJRE-G Classification: *FOR Code: 290502*

Strictly as per the compliance and regulations of:

A Theoretical Study of the Influence of the Injection Velocity on the Heat and Fluid Flow in A Soaking-Pit Furnace when using Flameless Oxyfuel Heating

Mersedeh Ghadamgahi [α], Patrik Ound [σ], Nils.A.I Andresson [ρ] & Par Jonsson [ω]

Abstract- Flameless oxyfuel combustion is one of the most recently developed combustion systems that has the potential to provide better combustion efficiency combined with a lower pollution production compared to conventional combustion systems. However, a lack of knowledge exists with respect to the influence of different parameters on the combustion results when using the flameless oxyfuel technology. Thus, in the current study a previously validated CFD model is used to investigate the effect of the injection velocity on the temperature distribution, recirculation ratio of the flue gases, flame volume, turbulence intensity, and flame radiation to the ingots. The results show that an increased injection velocity highly affects the temperature uniformity inside the chamber. More specifically, the maximum temperature difference in the flame region drops from 8.59% to 3.78% for burner capacities of 130 kW and 907 kW, respectively. The results also show that as the burner capacity is increased from 130 kW to 906 kW i) the flame volume increases from 0.02 m^3 to 2.6 m^3, ii) the turbulence intensity increases from 1.8% to 16% and iii) the recirculation factor increases from 1.77 to 2.03.

Keywords: soaking PIT furnace, CFD, oxy-fuel combustion, flame, heat transfer.

I. Introduction

In the process of producing steel and billets from scrap iron, the soaking pit furnaces are used to preheat the cast ingots after the casting process to provide for optimum temperature conditions before the rolling process. The latter process provides the desired metallurgical properties in the final products, so the input conditions for the rolling process are important. Therefore, the operational condition of the soaking process such as the efficiency of the combustion, uniformity of temperature and heat transfer, flame shape and flue gas composition largely influences the total energy consumption and pollution generation.

One promising method to control the pollution and to increase the combustion efficiency is to replace the air by a pure oxygen gas as the oxidant. This method was investigated intensely by International Flame Research Foundation (IFRF), where they focused on different aspects such as the measuring equipment, combustion characterization, CFD development and validation (1).

Examples of studies on the subject include the study of Buhre et al. (2) in 2015 and the study by Kim, et al (3) in 2007. More specifically, Buhre et al. (2) studied the effect of employing the oxyfuel systems as a method for CO_2 sequestration (2). Furthermore, Kim, et al (3) investigated the effect of oxyfuel combustion with external flue gas recirculation systems on the NO emission, based on an experimental work. They also investigated the oxyfuel burner flame stability for different external recirculation rates (3).

Wall et al. (4) also studied the effect of the gas recirculation inside the flame region on combustion. They concluded that the gas recirculation controls the flame temperature and flow pattern of the flue gases (4). In another experimental study, Andersson et al. (5) compared the combustion chemistry in conventional air-fuel combustion with the oxyfuel burner combustion. They concluded that the oxyfuel combustion system produces up to 30% less NOx emissions in comparison to the identical air combustion system (5). In 2010, Toftegaard et al. (6) carried out a comprehensive literature study on the subject of oxyfuel combustion and claimed that a big lack of research existed in the area (6). Beside this study, many numerical investigations were also published to study oxyfuel combustion (7) (8) (9). Also, many studies were focused on validating suitable CFD models to use for simulating the complicated case of oxyfuel combustion. In 2010, Johansson et al. (7) studied the effect of different radiation models on combustion when using oxyfuel burners and they compared predicted and measured data. More specifically, they studied special radiative characterization of flue gases in oxyfuel combustion and concluded that the Weighted Sum of the Gray Gases Model (WSGGM) is the most relevant radiation model to use(7). In 2012, Hjärtstam et al. (8) also carried out work to validate radiation models used to simulate oxyfuel combustion. They concluded that the gray-gas model is not sufficiently accurate to be used for this purposes compared to the non-gray gases model (8). In 2013, an

Author α: KTH Royal Institute of Technology. e-mail: mersedeh@kth.se

investigation on a suitable combustion model was also enrolled by Galletti et al. (10). They reported that if it is necessary to consider a fast chemistry this will significantly reduce the accuracy in predicting the temperature when using oxyfuel combustion (10).

In general, many advantages are associated with using oxyfuel combustion compared to air-combustion. These include a higher productivity, a higher flame temperature and thermal efficiency, a better radiative characterization of the flue gases, lower exhaust gases volume, and improved flame stability (11).

As the industry has started to use this combustion system, some practical issues have also observed. Mainly the issues were concerning the high NOx production, in case of air leakage into the combustion chamber. This emphasized that the lack of convective effects and high local temperature leads to the production of thermal NOx in industrial applications. This issue is extensively described in the work by Fredriksson at al. (12). They studied the effect of air leakage on the total NOx formation and reported that the sharp temperature gradient in the flame area produces a large amount of NOx during the combustion. Buhre et al. (2) also investigated some issues associated with the use of oxyfuel combustion with respect to the heat transfer, flame stability and gaseous emissions (2). Since the formation rate of thermal NOx is an exponential function of the flame temperature and a square root function of the oxygen concentration, it can be extremely reduced by controlling the flame temperature or by diluting it (13).

Based on the above described drawbacks with the oxyfuel combustion technology, a modified burner design was introduced by IFRF, namely the flameless oxyfuel technology (14). In this combustion system, a high Internal Flue Gase Recirculation (IFGR) is forced to the system to produce a leaner combusting mixture. The idea is to produce a low concentration of reactant so that the combustion is not initiated before the mixing process is completed (15). After reaching the auto-ignition temperature within the mixture, reactions takes place in a diluted manner. The flame in such combustion systems is very spread as well as it is invisible to the naked eye. This type of combustion, which can be implemented in both air oxidation combustion and oxyfuel combustion, is called flameless combustion (16).

The special aspects in these type of furnaces are two folded; an asymmetric and especial design of the injection nozzles, and very high (near-sonic) injection velocity of fuel and the oxidant. These aspects lead to the formation of a volumetric flame configuration that - in case of correct adjustments- results in a uniform temperature distribution and a lower local temperature within the flame. In this manner the high radiative bulk of flue gases turn into a volumetric flame which is the source of radiation inside the chamber (14).

Even though the flameless combustion technology is very young, it is already widely used in many industrial applications. Examples of applications in the steel industry are: walking beam and catenary furnaces at Outokumpu in Avesta, soaking pit furnaces at Ascometal , Rotary heart furnaces at ArceloMetal in Shelby, and soaking pit furnaces at Ovako Sweden AB, in Hofors (12).

This implies the necessity of filling the gaps of knowledge about this modern combustion technology, since there are very few studies done on the subject. In 2006, Vesterberg et al. (17) studied 10 full scale reheating and annealing furnaces equipped with flameless oxyfuel burners. They concluded that the use of this technology had many advantages such as: a more uniform heat transfer, a shorter heating time and consequently lower energy consumption, an ultra-low NOx formation. In addition, Krishnamurthy at al. (15) compared different combustion systems including flameless oxyfuel and High Temperature Air Combustion (HiTAC) burners with respect to their thermal efficiency, in-flame temperature distribution, heat flux, gas composition and NOx emissions (15). They used a semi-industrial furnace equipped with flameless oxyfuel burners. These results were later used by Ghadamgahi et al. (18) to validate a CFD model for modeling flameless oxyfuel combustion in a soaking pit furnace equipped with flameless oxyfuel burner in Ovako Sweden AB.

In this study, the previously validated CFD model (18) is used to investigate the effect of the burner capacity on the temperature distribution profile, radiation profile and the overall operational conditions of the combustion system.

II. Mathematical Modeling

A 3-dimentional mathematical model was developed to simulate the combustion and turbulence by using Ansys Fluent 16.0. The equations were solved by considering the system to be in a steady state. It was also assumed that the flue gas mixture behaved like a perfect gas mixture. The following governing equations were solved:

Based on these assumptions, the following governing equations were solved:

Continuity equation:

$$\nabla.(\rho\,\mathbf{u}) = 0 \tag{1}$$

Momentum equation:

$$\nabla.(\rho\,\mathbf{u}\,\mathbf{u}) = -\nabla p + \nabla.(\bar{\bar{\tau}}) + \rho\boldsymbol{g} \tag{2}$$

Energy balance equation:

$$\rho c_p \mathbf{u}.\nabla T = \nabla.(k\nabla T) + S_h \tag{3}$$

where $\mathbf{u}$ is the velocity vector (m/s), ρ is the density (kg/m3) and $\bar{\bar{\tau}}$ is the stress tensor. Furthermore, $\rho\mathbf{g}$ and $\mathbf{p}$ are the gravitational body forces and the pressure (Pa), respectively. In addition, $\mathbf{k}$ represents the thermal conductivity (W/m·K), and $\mathbf{c_p}$ defines the heat capacity at a constant pressure (J/kg·K) [26]. Also S_h counts for any volumetric heat sources.

Regarding the incompressible behaviour of the flow, the Navier Stokes equation is solved, which can be written as follows:

$$(\mathbf{u}.\nabla)\mathbf{u} - \nu\nabla^2\mathbf{u} = -\nabla\omega + \boldsymbol{g} \qquad (4)$$

where the parameter $\mathbf{g}$ represents the gravity and ω is thermodynamic work on the system. Furthermore, the parameter $\nu = \frac{\mu}{\rho}$ is the kinematic viscosity (18).

The flow was assumed to be fully turbulent, incompressible and the diffusion coefficients for all the gaseous products were assumed to be equal. Therefore, turbulence was modeled by using a Realizable k-ε turbulence model to solve the Navier-Stokes equations. This selection of the sub-model is extensively explained in the work by Ghadamgahi et al. (19). However, it can briefly be stated that in this model the kinetic energy (k) and the turbulent dissipation rate (ε) were solved as shown in equation 5 and equation 6:

$$\frac{\partial(\rho k)}{\partial t} + \frac{\partial(\rho k u_i)}{\partial x_i} = \frac{\partial}{\partial x_j}\left[\left(\mu + \frac{\mu_t}{\sigma_k}\right)\frac{\partial k}{\partial x_j}\right] + G_k + G_b - \rho\varepsilon \qquad (5)$$

$$\frac{\partial(\rho\varepsilon)}{\partial t} + \frac{\partial(\rho\varepsilon u_j)}{\partial x_j} = \frac{\partial}{\partial x_j}\left[\left(\mu + \frac{\mu_t}{\sigma_\epsilon}\right)\frac{\partial\varepsilon}{\partial x_j}\right] + \rho\, C_1 S_\varepsilon - \rho C_2 \frac{\varepsilon^2}{k+\sqrt{\nu\varepsilon}}] + C_{1\varepsilon}\frac{\varepsilon}{k}C_{3\varepsilon}G_b \qquad (6)$$

Where $C_1 = \max\left[0.43, \frac{\eta}{\eta+5}\right]$, $\eta = S\frac{k}{\varepsilon}$, $S = \sqrt{2S_{ij}S_{ij}}$ And $\sigma_k = 1.0$, $\sigma_\varepsilon = 1.2$, $C_2 = 1.9$, $C_{1\varepsilon} = 1.44$ and $C_{3\epsilon}$ is described by equation (7).

$$\boldsymbol{C_{3\epsilon}} = \mathbf{tanh}\left|\frac{v_\parallel}{u_\perp}\right| \qquad (6)$$

The combustion was solved by using a SLFM to solve the PDF. The developed model also treats the combustion chemistry, departed from the chemical equilibrium, which is a necessary consideration in modeling flameless combustion systems (19). In this mathematical solution, the thermochemistry parameters are a function of both the mixture fraction and the dissipation rate ($\boldsymbol{\chi}$), which are described in equations 7 and 8, respectively.

$$f = \frac{Z_i - Z_{i,ox}}{Z_{i,fuel} - Z_{i,ox}} \qquad (7)$$

$$\chi = 2D|\nabla f|^2 \qquad (8)$$

where D is the diffusion coefficient.

It is important to note that in this study the infiltration of air was assumed to be negligible and NO_x products were not considered.

The radiative Transfer Equation (RTE) was solved, using the DO model. In oxyfuel combustion systems the flue gas radiative properties are strongly promoted compared to conventional air-fuel combustions. It is also unsatisfactory for the predictions to consider the non-gray gas model (8). In this regards the WSGGM was also considered to count for the variation of the absorption coefficient of the flue gases. The accuracy of using his model in oxyfuel combustions has been investigated in many former studies (20) (21) (22) (23) (19). Also, the total emissivity over the distance $\vec{s}$ can be presented as follows (24):

$$\varepsilon = \sum_{i=0}^{I} a_{\epsilon,i}(T)(1 - e^{-k_i ps}) \qquad (9)$$

where $a_{\epsilon,i}$ stands for the emissivity weighting factor for the *i*:th fictitious gray gas and the quantity in the bracket stands for the i^{th} fictitious gray gas emissivity. Furthermore, k_i is the absorption coefficient of the i^{th} gray gas, *p* is the summation of the partial pressure of all absorbing gases, and *s* is the path length (19).

III. Materials and Methods

a) Soaking pit furnace

The experimental work that has been done on a soaking pit furnace in Ovako Sweden AB, is extensively described in refernces *(18)* and *(25)*. These furnaces are used to provide preheating on the ingots in order to prepare them for the rolling process. The furnaces are made of four cells which have a rectangular shape with a total volume of 14.11 m^3 . Figure 1 shows the configuration of one cell including the ingots. Each cell accomodates 6 ingots that seat inside the chamber with the aid of automatic hooks. During the heating, the soaking time and soaking temperature are essencial parameters, that are set corresponding to the special type of the steel grade and the desired final steel properties *(18)*.

The soaking pit furnaces in Ovako Sweden AB, are all equipped with REBOX® flameless oxyfuel burners that uses pure oxygen as the oxidant and LPG No.95 as the fuel *(18)*. The injection velocity of the fuel and oxygen may easily be adjusted by the operators. The maximum burner capacity is 900 kW. However, in the soaking pit furnaces in Ovako, a lower amount (560 kW) is used to accomplish a flamelss oxyfuel combustion. This burner is mounted on the frontal wall

of the chamber, where both the controlling thermocouple and the exhaust channel are located. The controlling thermocouple is located 400 mm below the center of the burner and it continuously monitors the temperature *(18)*.

The quality of operational conditions of the furnace has a major effect on the soaking cost and quality. Especifically factors such as the temperature and heat transfer uniformity inside the chamber, the level of pollution production, and combustion efficiency determines the overal state of the furnace effectiveness. The refractory walls are made of 230 mm AK60 A, 115 mm Porosil and Skamolex 1100 in 450 and 200 mm at the transverse and longitudinal walls, respectively.

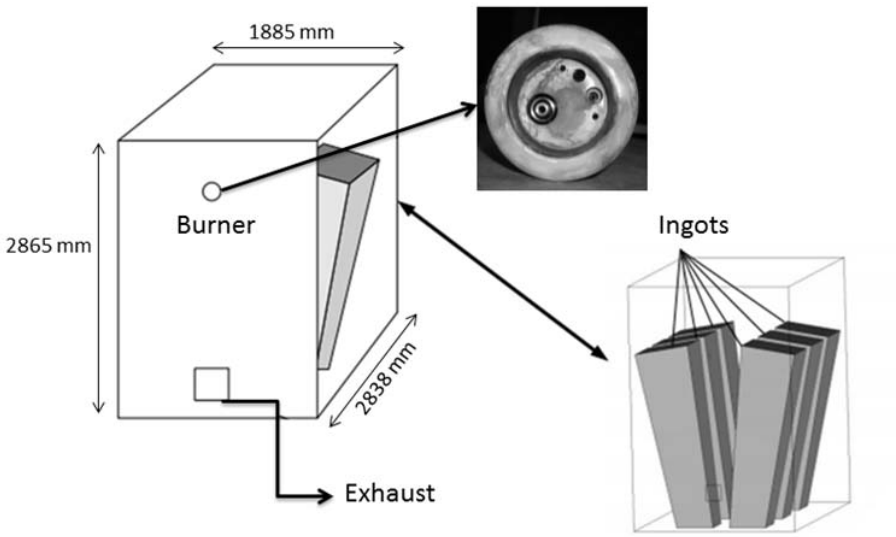

Figure 1: Soaking pit furnace configuration and arrangement of ingots inside the furnace (18)

b) Experimental Work

The experimental work which has been done in Ovako Sweden AB, is explained in detail in the work by Ghadamgahi et al. *(18)*. For the experimental result used in th ecurrent study the local temperature of the flue gases was measured by using shielded S-type thermocouples. In addition, the locations of the sampling was carefully selected to provide a comprehensive view of the temperature profile inside the chamber. Overall, eight thermocouples were inserted to the furnace from the top side. These were divided in two different groups that were located at two different levels inside the chamber. These levels are called the High and Low levels, which are located at the heights of 2016 mm and 1065 mm, respectively. The exact position of the probes are given in Table 2 and the configuration is illustrated in figure 2 *(18)*.

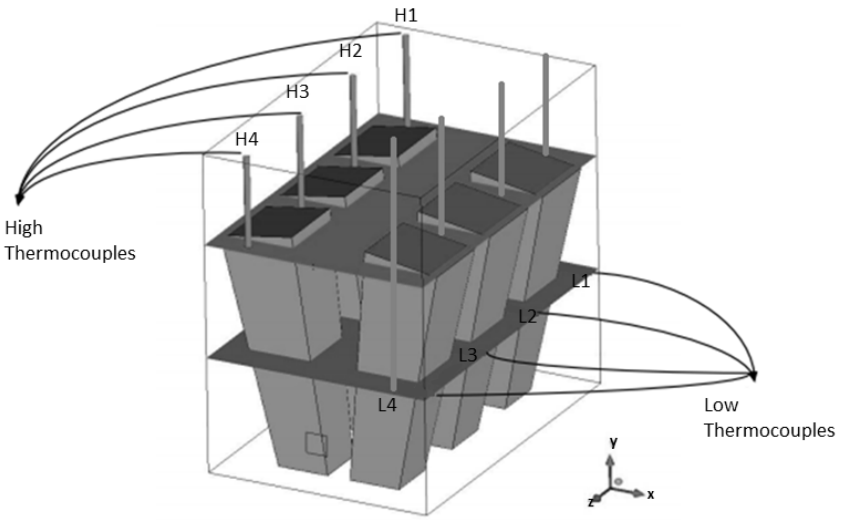

Figure 2: Rrangement of thermocouples in the soaking pit furnace (18)

Table 2: Coordinates of the S-types thermocouples inside the soaking pit furnace (18)

Thermocouple	Ref.	Low1	High1	Low2	High2	Low3	High3	Low4	High4
X (mm)	910	1487	514	1487	514	1487	514	1487	514
Y (mm)	1105	1065	2065	1065	2065	1065	2065	1065	2065
Z(mm)	0	2631	2631	1810	1810	987	987	246	246

c) *Geometry and mesh*

ICEM 13 was used to draw the geometry of the furnace as well as the mesh structure. Note, that the configuration of the ingots inside the chamber is simplified in this scheme compared to the original arrangement. More specifically, the ingots were assumed to be standing up in the chamber and therefore the effect of leaning them towards the walls was neglected. This helps to decrease the number of nodes from 980000 to 850000, which consequently reduces the computational costs *(25)*.

A study on the grid independancy of the mesh was also done *(18)* by observing the results of the simulation from two mesh configurations, namely tetragonal mesh and hexagonal mesh. The unstructured tetrahedron mesh with a combination of the O-rings (Figure 3) for the inlet area was reported to be the best choice, regarding both the time required for a converged solution and an acceptable prediction accuracy *(25)*. Also, the minimum orthogonal quality was 0.84, which is adequate according to the previously presented results *(18) (19)*.

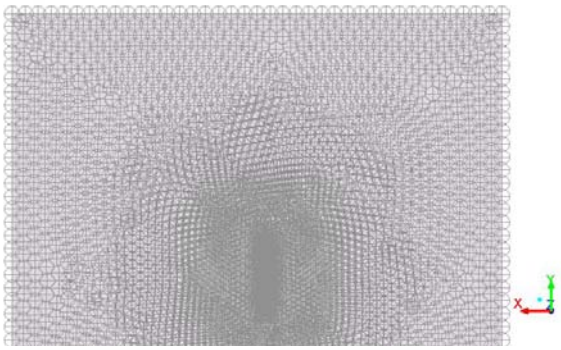

Figure 3: Unstructured mesh and O-rings located at the frontal face

d) *Boundary conditions*

The boundary conditions for the reference case at the inlets are shown in Table 1. These data are taken from the operational conditions of the furnace at the plant. They were used in the simulations made by Ghadamgahi et al. **(18)** in order to validate sub-models for simulating the flameless oxyfuel burner at Ovako Sweden AB.

Table 1: Inlet boundary conditions for the reference model. (18)

Parameter	Propane	Oxygen
Mass Flow (kg/s)	0.013	0.06
Inlet temperature (°C)	22	25
Hydraulic Diameter (mm)	7	5
Turbulent Intensity (%)	5	6

In order to study the role of the burner capacity on the combustion, six cases with different inlet boundary conditions were simulated. The burner capacity in these cases gradually increased from 130 kW in case 1 to 907 kW in case 6. Also, the mass rate for fuel and oxygen was calculated according to the corresponding burner capacity by assuming a constant lambda value for all the cases. These data are shown in Table 2.

Table 2: Inlet boundary condition for the different cases in this study

Case Number	Inlet Fuel Rate (Kg/s)	Inlet Oxygen Rate (Kg/s)	λ	Burner Capacity(KW)
CASE 1	0.002	0.0074	1.02	130
CASE 2	0.005	0.0185	1.02	259
CASE 3	0.008	0.0296	1.02	389
CASE 4	0.011	0.0407	1.02	518

CASE 2	0.005	0.0185	1.02	259
CASE 3	0.008	0.0296	1.02	389
CASE 4	0.011	0.0407	1.02	518
CASE 5	0.016	0.0592	1.02	777
CASE 6	0.019	0.0703	1.02	907

It is important to note that the mentioned inlet boundary conditions are used to demonstrate that the flameless oxyfuel mode, which is applied after the chamber, reaches the self-ignition temperature.

In the simulation, fuel and oxygen are not preheated and therefore they enter the chamber at 22°C and 25°C, respectively. Also, the refractories are defined as heat sinks with constant heat fluxes. These magnitudes are computed regarding the material of the .

Table 3: Heat flux boundary condition parameters for the exterior walls (18)

Layer	Bottom	Longitudinal wall	Transversal wall	Lid
Heat loss (W/m²)	530	450	500	650

The ingots are also considered as heat sinks, with a separate constant heat flux for each ingot. The procedure of calculating these magnitudes is extensively explained in the work by Ghadamgahi et al. (18). In this study, the total heat flux on each ingot was predicted by assuming a fixed temperature for each of the ingots during the entire heating period. The final magnitudes for all the ingots are shown in Table 4 (18). The ingots' marking is illustrated in Figure 4.

Table 4: Wall boundary conditions for the ingots. (18)

Ingot	Heat flux (kW/m²)
Ingot 1 (Front-right)	56.7
Ingot 2 (Middle-right)	43.7
Ingot 3 (Rear-right)	61.0
Ingot 4 (Front-left)	45.2
Ingot 5 (Middle-left)	48.4
Ingot 6 (Rear-left)	65.1

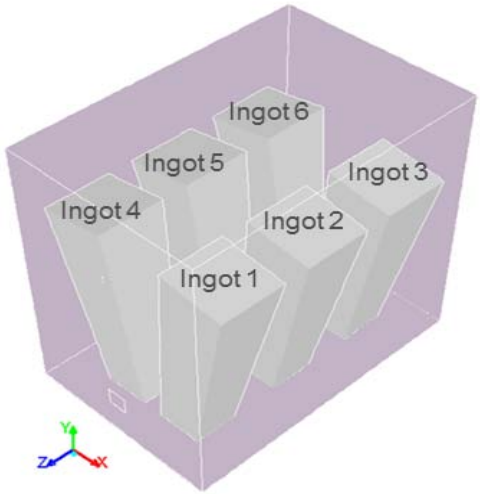

Figure 4: The marking of the ingots located in the soaking-pit furnace cell

IV. Results and Discussions

a) Validation

In this section, the results of simulation and experiments done by Ghadamgahi et al. *(18)* are used to show that the sub-models used in this study have been previously validated. The maximum deviation between the predicted results and experimental results, for all the thermocouples (High and Low) are shown in Table 5. The experimental work was done at the plant in Ovako Sweden AB, using a real-size soaking pit furnace *(18)*.

Table 5: Maximum deviation between the CFD predictions and experimental data (18)

Thermocouple positions	Experimental Temperature (°C)	Predicted Temperature (°C)	% Deviation
High 1	1366	1230	9.95 %
High 2	1264	1220	3.48 %
High 3	1236	1119	3.47 %
High 4	1239	1193	3.71 %
Low 1	1320	1195	9.46%
Low 2	1277	1173	8.14%
Low 3	1225	1155	5.71%
Low 4	1206	1176	2.48

As shown in the table 5, the deviations between the predicted and measured temperatures varied between 3.47% and 9.95 %, which is considered to be fairly small for this type of furnace. Thus, the authors feel comfortable that the model can be used to make reliable predictions of temperatures in soaking pit furnaces.

b) Temperature Distribution And IFGR

An increase of the burner capacity when using flameless oxyfuel burner combustion highly affects the temperature distribution, flame shape and the flame temperature. Figure 5 shows the results for predicted temperature at the centerline of the furnace for all the studied cases. The line of representation starts from the burner face on the frontal side and ends at a position of 2000 mm from the back-wall.

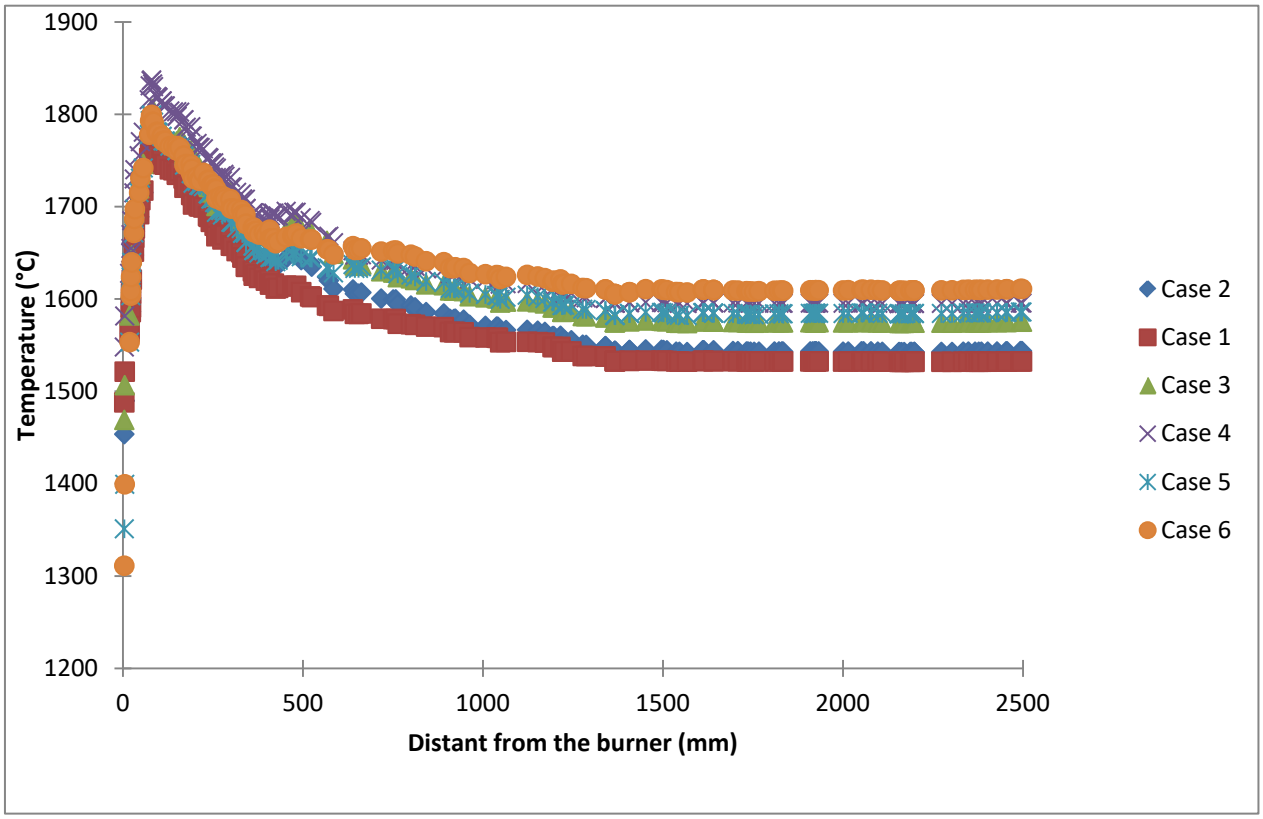

Figure 5: Local temperature in the flame region shown at a distance starting from the burner and ending on the back-wall

A very rapid increment for temperature is seen in regions very close to the burner side, which stands for the formation of the reaction zone for all the cases. This is followed by a rapid decrement for the temperature values at a distance of 500mm from the burner.

The maximum temperature in the flame region is highly dependent on the injection velocity. More specifically, this temperature is increasing while moving from case 1 with 130 kW to case 4 with 518 kW (1785 °C to 1820 °C). Afterwards, this temperature is decreasing from case 4 with 518 kW (1820 °C) to case 5 with 717 kW (1812 °C) and case 6 with 907 kW (1799 °C). Also, the maximum difference (between the peak and chamber temperature) for cases1, 2 and 3 are 255°C, 242 °C and 235°C, respectively. This magnitude for cases 5 and 6 is seen to be 172 °C and 149 °C, which is considerably smaller compared to the other cases. Figure 6 shows the magnitudes of these values with respect to the percentage of the temperature deviation at the centerline.

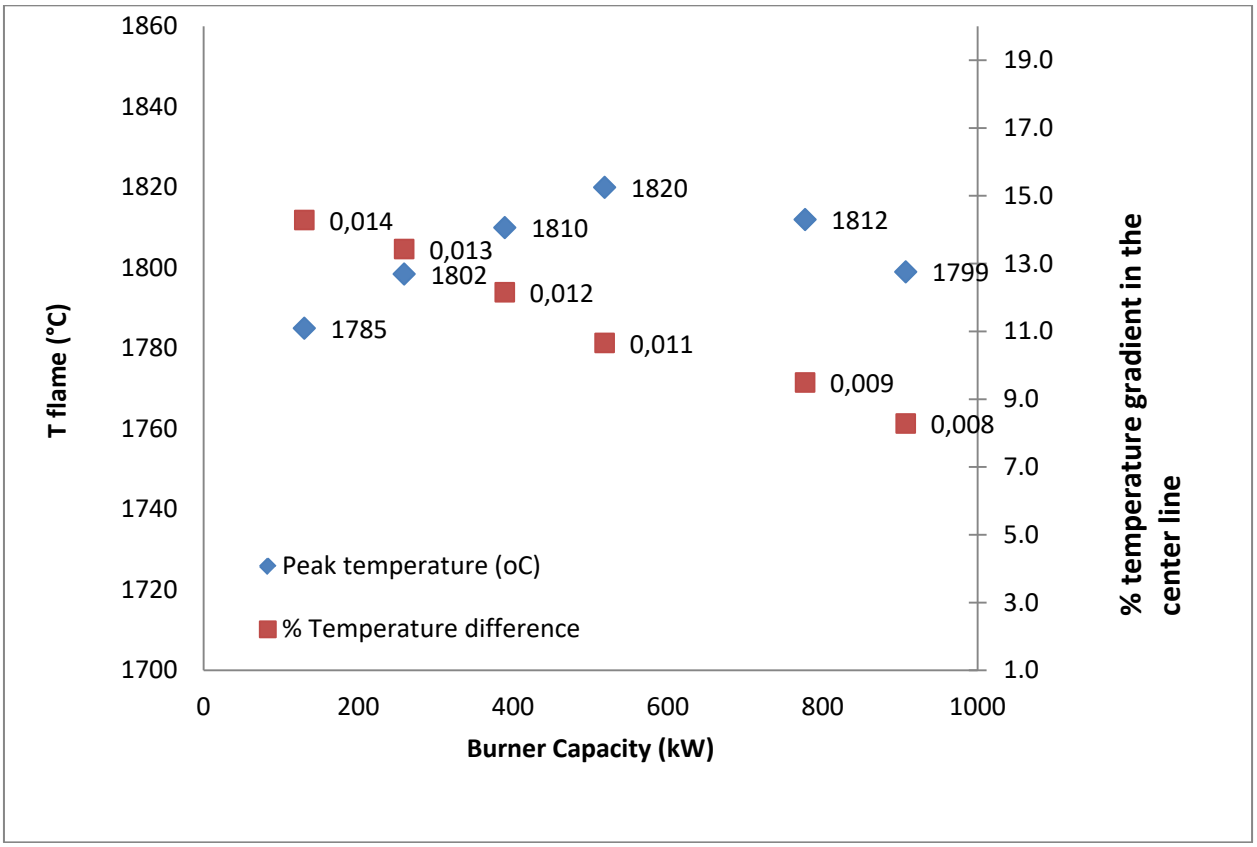

Figure 6: Predicted flame temperature (right axis) and the percentage of predicted temperature difference (left axis) at the centerline of the furnace

This figure indicates that the temperature uniformity is improved by increasing the inlet velocities of oxygen and fuel, as the temperature difference on the centerline decreases from 13% for case 2 to 8 % for case 6. This velocity increase leads to formation of a leaner reacting mixture and lower concentration of O_2 with a colder but more uniform flame. These results also show the effect of higher velocity on reducing the flame temperature in cases 5 and 6, which is in good agreement with the work done by Milani et al (26). Also in 2016, Ghadamgahi et al. (25) reported results on the influence of the lambda value on the operational conditions in form of increasing the inlet oxygen mass rate. More specifically, they looked into the effect of increasing inlet velocities on the temperature distribution and consequently the exhaust losses. They also reported that although an increased oxygen velocity leads to a larger exhaust loss by 9.2%, it improves the temperature uniformity by 28%.

In order to further study the relevance between a total increase of the burner capacity and flame characterization, Figure 7 Shows the temperature distribution profile for the selected cases of 1, 2, 5 and 6 at a middle plane on a z-y axis.

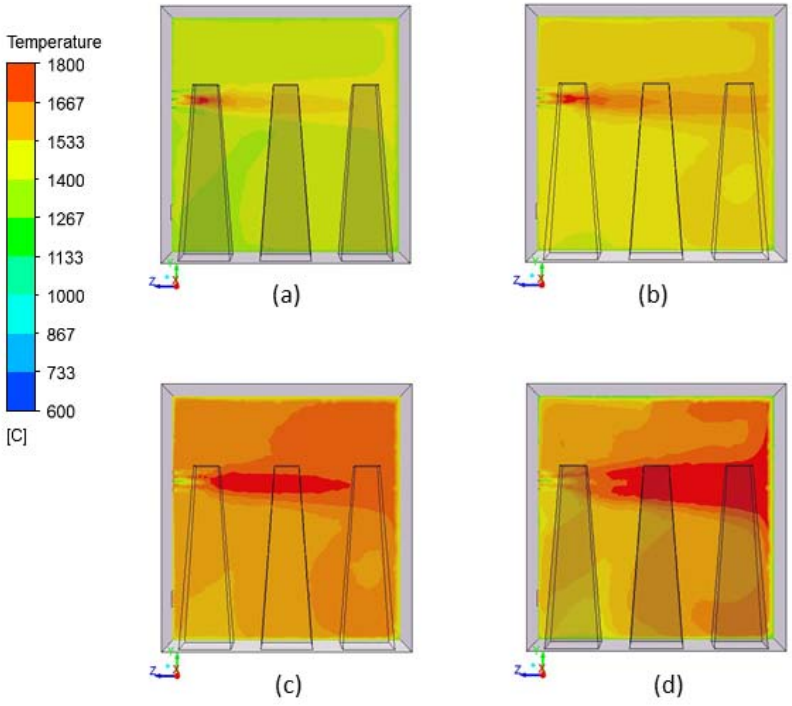

Figure 7: Temperature distribution profile for the following cases: (a) Case 1, (b) Case 3,(c) Case 5 and (d) Case 6 on a plane located in the middle of the z-y axis

As it is shown in Figure 7, an increase of the injection velocities leads to the formation of a more turbulent mixing flow and a better recirculation of gases inside the chamber. In Case 3, especially in areas with fluid impinging effect, a wider range of temperature spectrum (temperature difference of 422°C) on this z-y plane is seen . Although a less temperature difference exists in case 6 (384°C), due to formation of large eddies and turbulence intensity. Figure 8 shows the predicted values of the turbulence intensity (%) for all the cases, in the length of the chamber.

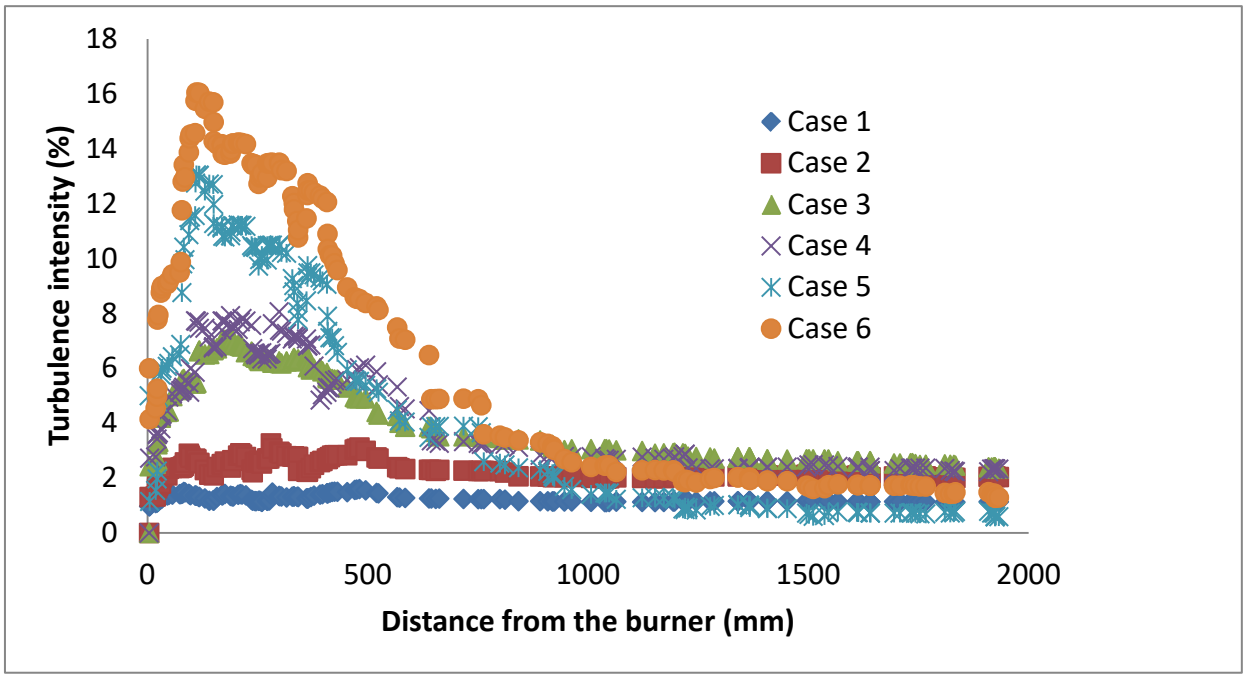

Figure 8: The turbulent intensity of the flow on an axial line for cases 1 to 6

As shown in Figure 8, turbulence intensity dramatically increases with an increased injection velocity, in the flame region (50-400 mm away from the burner). This effect, which is in line with the predicted results for temperature, shows the effect of turbulence in making a more uniform temperature distribution. Additionally, Figure 9 shows the temperature profile on an x-z plane in the middle of the furnace. A higher degree of volumetric flame is expected to form by going from case 1 to 6 (increasing injection velocities), according to the results in this figure. However, the flame impinging effect on the rear wall suppresses this effect due to the chamber configuration. In the previous studies brought in sections 5 and 6 (supplements 2 and 3) the effect of a flame impingement on the temperature distribution was argued. Although this effect is neglected in this study, as Figure 8 reports the turbulence far away from the impinging side.

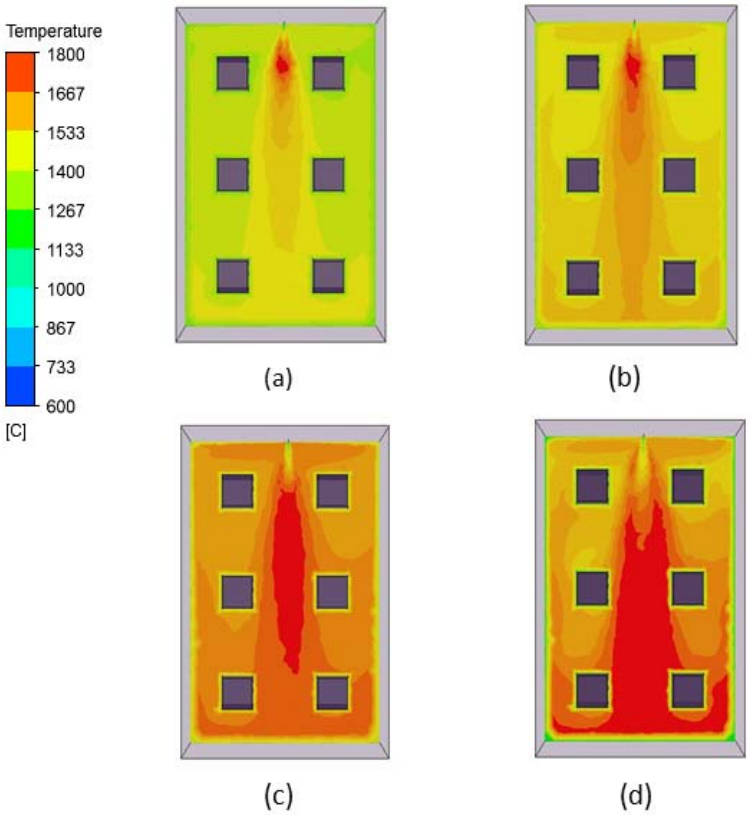

Figure 7: Temperature distribution profile for the following cases: (a).case 1,(b).case 3,(c).Case 5 and (d).Case 6 on a plane located in the middle of the x-z axis

In a flameless oxyfuel combustion, the chemical reactions happens with departure from chemical equilibrium, since the gas mixture of the reactants is leaned with recirculated flue gases. This is due to that the IFGR inside the chamber in the neighborhood of the flame region is increased (26). In this regard one of the most important factors for determining the flameless behavior of the combustion is the value of the recycle ratio of the combusting gases. This value was introduced by Hasegawa et al. (27) as:

$$k_v = \frac{M_e}{M_a + M_f} \qquad (10)$$

where $M_e$is the internal exhaust gases flow rate that is recirculated into the mixing reactants before a reaction takes place. Furthermore, $M_a$is the combustion oxygen flow rate, and M_f is the fuel flow rate. Combustion is conventionally stable for $k_v < 0.3$, although for $k_v > 0.3$ temperature of the furnace determines the stability of the flame (3). Higher recirculation of the flue gases threatens the flame stability and can even result in a flame lift-up and a blow-out case of a chamber temperature lower than the self-ignition temperature (29). Therefore, using a stable combustion with a high IFGR value is only beneficial in case of a sufficiently high temperature in the chamber (reactants temperature $> \sim$ 700 °C). This, on the other hand, stresses the necessity of defining a gradual combustion process in order to avoid to operate the burner in the flameless mode in a cold chamber.

c) Flame shape and total radiation on the ingots

Heat transfer inside the industrial furnaces is mainly carried out by two heat transfer methods, namely

radiation and convection. Naturally the most effective parameters that influence the heat transfer ratio are the: i) flame temperature, ii) flame shape and emissivity, iii) ingots' initial temperature and emissivity, and iv) the temperature and emissivity of the walls. Oxygen content in the oxidizer plays an essential role in the final radiative fluxes from the flue gases, since it attains the final radiative properties of the flue gases. More specifically, by using oxygen as the oxidant instead of air a significant increment in the total flue gas emissivity is obtained. It also causes a significant decrement in the total flue gas volume, compare to air-fuel combustion systems. Another special aspect of using flameless oxyfuel flames is the formation of a widespread flame shape with a lower peak temperature, as shown in Figure 8. This figure is taken from the work by Blasiak et al. (31) . This ideally turns the flame into a large radiation source that has a uniform temperature, which highly influences the uniformity of the heat transfer.

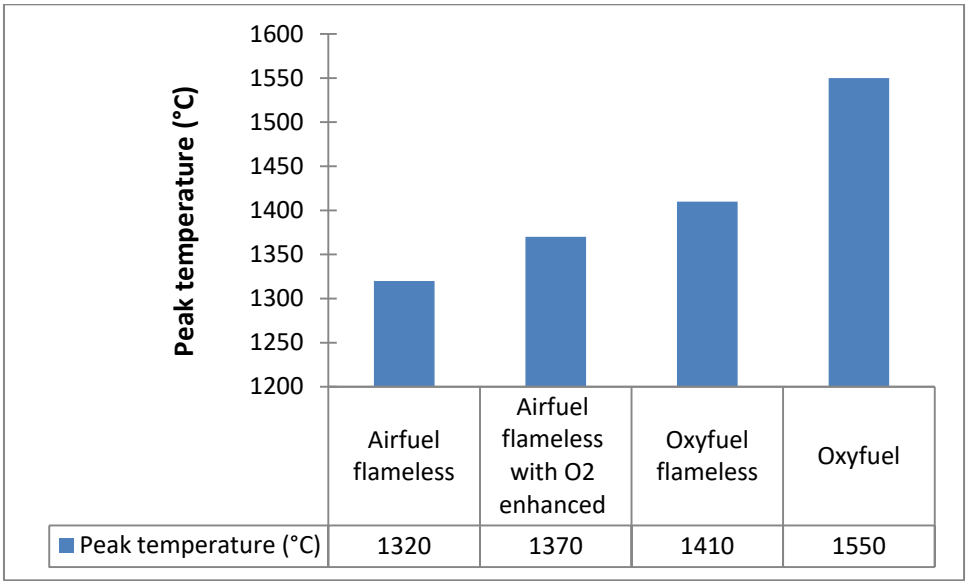

Figure 8: The peak temperature inside the flame region, for different burner configurations (31)

In 2007, Krishnamurthy et al. (13) developed a theoretical model that simply illustrates the radiation inside the industrial furnaces. This model is illustrated in Figure 9 and demonstrates the heat transfer exchange between the flame, the ingots and the furnace walls (15).

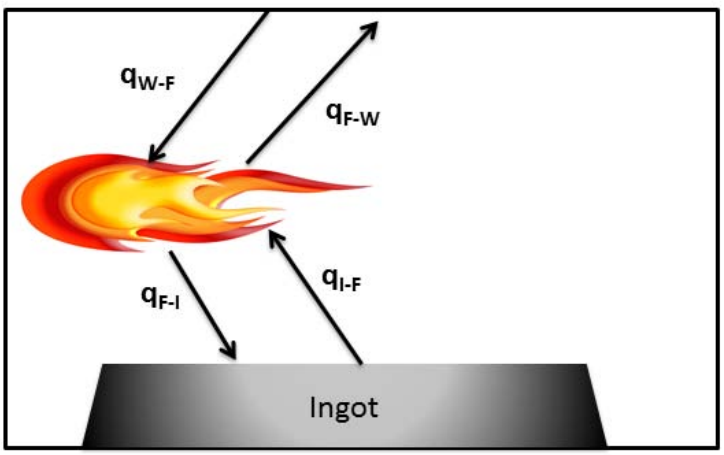

Figure 9: Radiation heat transfer inside a furnace

Overall, in flameless oxyfuel combustion flame has a lower temperature, but a more volumetric shape. These factors change the behavior of heat exchange between the flame and the ingots inside the chamber. Since the flame is the main radiation source, the heat is transferred to the slabs directly from the flame and indirectly from the walls. Thereby a net heat flux from the flame to ingots can be obtained from the following correlation (31):

$$q_{net} = q_{F-I} - q_{I-F} = \frac{A\sigma(T_F^4 - T_I^4) + B\sigma(T_W^4 - T_I^4)}{C} \qquad (16)$$

where

$$A = \varepsilon_I\varepsilon_F(2 - \varepsilon_F - \varepsilon_W + \varepsilon_W\varepsilon_F)$$
$$B = \varepsilon_I\varepsilon_W(1 - \varepsilon_F)$$
$$C = 1 - (1 - \varepsilon_F)^2(1 - \varepsilon_W)(1 - \varepsilon_I)$$

The subscripts F, I and W correspond to the flame, ingots and refractory wall respectively. Furthermore, T_w is the furnace wall temperature (K), T_F is the flame temperature (K), and T_I is the ingots' temperature (K). Finally, ε_W, ε_I and ε_F are the emissivity values of the walls, ingots and flame respectively. The parameter σ is the Stefan–Boltzmann constant. With the assumption of ε_F, ε_W and ε_I to be 0.25, 0.8 and 0.85, respectively, and assuming the flame having a cylindrical shape, the total heat transferred from the flame to the ingots (kW) can be described as follows (31):

$$Q_{net} = \left[\frac{A\sigma(T_F^4 - T_I^4) + B\sigma(T_W^4 - T_I^4)}{C}\right]\frac{4V_F}{d_F} \quad (19)$$

where V_F d_F and l_F stand for the flame volume, flame diameter and flame length, respectively. This equation illustrates the importance of the role of the wall temperature and flame temperature on the incident radiation on the ingots' surfaces. As if the combustion happens in a fameless manner, with a low and well-spread volume, the radiation is more uniform on the ingots. On the other hand, a high peak temperature in the flame area has an opposite effect. It can also be understood that having a flame impinging effect on a refractory wall and formation of a thick thermal boundary layer, makes that area a compacted radiative source that jeopardizes the radiation uniformity (32).

In order to investigate this effect, we consider the entire flame as a volumetric source of radiation to the surroundings. Thus, the radiated energy from the flame can be expressed as follows:

$$Q_{rad} \approx \alpha_F V_F \sigma T_F^4 \quad (20)$$

where α_F is the Planck mean absorption coefficient for an optically thin flame. This simplification leads us to the introduction of a known term *"D"*, based on the study done by Turns in 1996 (32). *D* is defined as the ratio of the radiant heat transfer rate from the flame to the surroundings (Q_{rad}) to the total heat released by the flame (Q_0), and it can be written as follows:

$$D = \frac{Q_{rad}}{Q_0} \approx \frac{\alpha_F V_F \sigma T_F^4}{Q_0} \quad (21)$$

This can lead us to the following function for the flame volume:

$$V_F \approx \frac{DQ_0}{\alpha_F \sigma T_F^4} \quad (22)$$

Figure 15 shows the relevance between the flame volume, Q_{rad} and D , for all the studied cases.

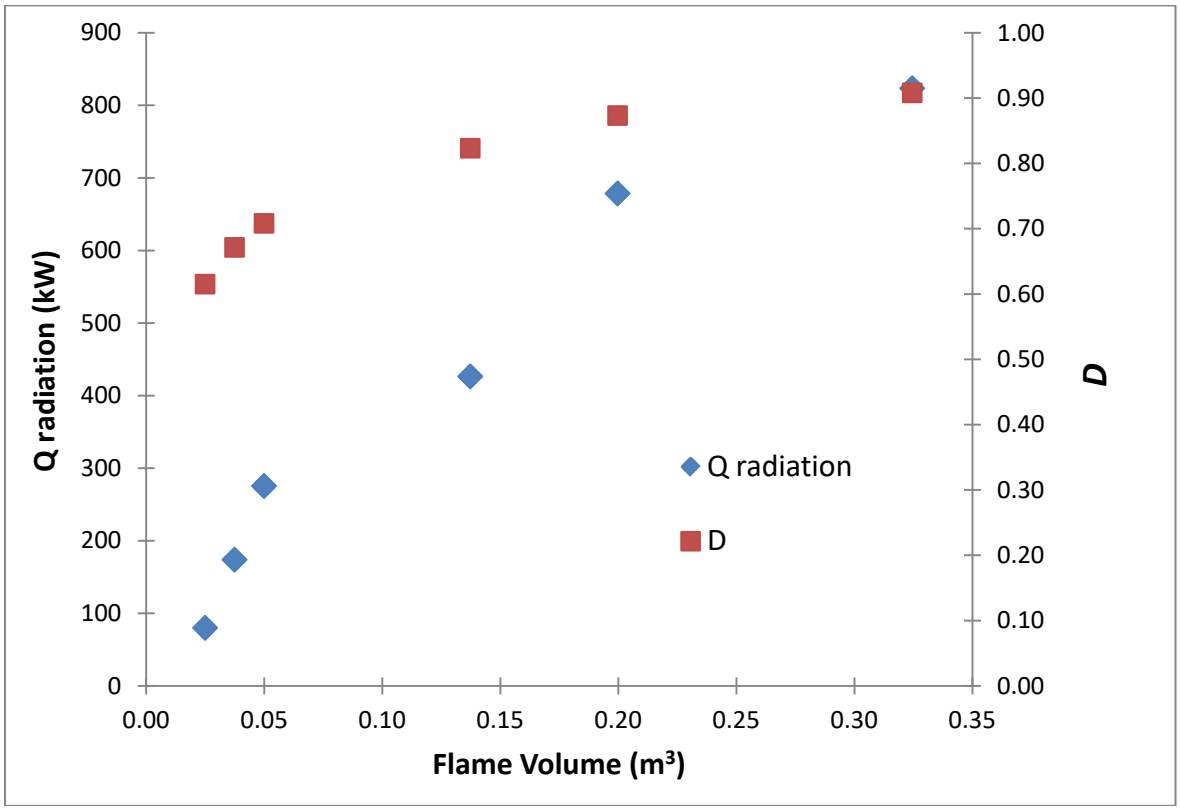

Figure 15: The ratio of the radiant heat transfer rate from the flame to the surroundings and total radiation flux (kW) as a function of the flame volume (m^3)

This figure demonstrates the effect of flame volume on total radiation, meaning an increased flame volume increases the total radiation from the flame. It is also seen that the increase in the ratio between the radiative heat transfer and total released heat from the flame loses its significance after a radiation value of 700 kW. This calculation is done by assuming a 100% combustion efficiency.

In a general view, with the increase of flame volume, temperature drops, but total radiation heat flux increases (31). In 2007, Blasiak et al. (31) carried out the same calculations with the focus on studying the effect of gas emissivity and flame volume on the total heat transfer. They concluded that when the gas temperature distribution inside the furnace chamber (well stirred reactor) is uniform, the effect of the flame emissivity becomes smaller than the effect of the flame volume (31).

V. Conclusions

The aim in the current study was to simulate flameless oxyfuel combustion using a previously validated CFD model. More specifically, the focus was to investigate the effect of the injection velocity on the temperature distribution, flame temperature, flame volume, turbulence intensity, and flame radiation to the ingots. Based on the results of this study, the following main conclusions may be drawn:

- An increase of the injection velocity highly affects the flame temperature and temperature uniformity inside the chamber as the maximum temperature difference in the flame region drops from 14% to 8% for burner capacities of 130 kW and 907 kW, respectively.
- The formation of a more uniform temperature profile when using a higher burner capacity of 907 kW instead of a 130 kW capacity is due to the formation of a more volumetric flame. This, in turn, leads to the formation of a more turbulent flow and increased recirculation ratio of the flue gases in the reacting zone.
- An increased burner capacity from 130 kW to 906 kW leads to an increase of the flame volume from 0.02 m^3 to 2.6 m^3, an increase of the turbulence intensity from 1.8% to 16%.
- With an increase of flame volume from case 1 to case 6, temperature drops, but total radiation heat flux increases.
- The radiation from the flame to the ingots increases from 79.9 kW to 823.5 kW and the Q_{net}/Q_0 ratio increases from 0.36 to 0.85 with an increased burner capacity from 130 kW to 906 kW.

Bibliography

1. *Analysis of theexperimental data collected during the oxyflam-1 andoxyflam-2 experiments* IFRF DocNo. F85/y/4
2. *Oxy-fuel combustion technology for coal-fired power generation* 4Progress in Energy and Combustion Science
3. *NO reduction in 0.03–0.2 MW oxy-fuel combustor using flue gas recirculation technology* Proceedings of the Combustion Institute
4. *Oxy-fuel (O2/CO2, O2/RFG)* the 30th international technical conference on coal tilization &fuel systems2005
5. *NO Emission during Oxy-Fuel Combustion of Lignite* Industrial and Engineering Chemistry research
6. *Oxy-fuel combustion of solid fuels* Progress in Energy and Combustion Science
7. *Models for gaseous radiative heat transfer applied to oxy-fuel conditions in boilers* 1-3International Journal of Heat and Mass Transfer
8. *Computational Fluid Dynamics Modeling of Oxy-Fuel Flames: The Role of Soot and Gas Radiation* 5energy and fuels
9. *Experimental and numerical investigations on a swirl oxy-coal flame* Applied Thermal Engineering
10. *Numerical investigation of oxy-natural-gas combustion in a semi-industrial furnace: Validation of CFD sub-models* Fuel
11. *Oxygen-Enhanced Combustion*CRC Press1998
12. *Application of oxyfuel combustion in reheating at Ovako,Hofors works, Sweden – Background, solutions and results* Linde AGA2006
13. *Flameless oxyfuel combustion: technology* La Revue de Métallurgie-CIT
14. *Flameless oxyfuel combustion for increased production and reduced CO2 and NOx emissions*Stahl und eisen 1282008
15. *Studies on low-intensity oxy-fuel burner* Proceedings of the combustion Institute
16. *Mild Combustion* 4Progress in Energy and Combustion Science
17. *Flameless oxyfuel for highly visible results* Cleveland,AISTech 20062006
18. *Numerical and Experimental study on flameless oxy-fuel combustion in a pilot-scale and a real-size industrial furnace* Submitted to : Appiled thermal engineering
19. *A Comparative CFD Study On Simulating Flameless Oxy-fuel Combustion In A Pilot-scale Furnace* StockholmJournal of Combustion6735971
20. *Numerical Simulation of Properties of a LPG Flame with High-Temperature Air* Thermal Sciences
21. *Chemistry and radiation in oxy-fuel combustion: A computational fluid* fuel
22. *Experimental and numerical investigations on a swirl oxycoal flame* Applied Thermal Engineering

23. *Design Optimization of Flameless-oxyfuel Soaking Pit Furnace Using CFD Technique* Energy Procedia
24. *Radiative Heat Transfer*Academic Press2013ISBN: 978-0-12-386944-9
25. *Numerical study on the effect of lambda value on temperature distribution and efficiency of a flameless oxyfuel combustion system* Submitted to "Energies"
26. *Laseroptical investigation of highly preheated combustion with strong exhaust gas recirculation* Proceedings of combustion institute
27. *Combustion with High Temperature Low Oxygen Air in Regenerative Burner* Osaka, JapanAsia-Pacific Conference on Combustion1997
28. *The Role of Exhaust Gas Recirculation in flameless combustion* Applied mechanics and materials
29. *Mild combustion in a laboratory-scale apparatus* Combustion Science and Technology
30. *Flameless oxidation to reduce thermal NO-formation* Prog. Energy Combust. Sci
31. *Flameless oxyfuel combustion for fuel consumption and nitrogen oxides emissions reductions and productivity increase* Energy institutes
32. *An Introduction to Combustion: Concepts and Applications*New York : McGraw-Hill1996
33. *Nongray-Gas Effects in Modeling of Large-Scale Oxy–Fuel Combustion Processes* 6Enertgy and fuels
34. *Numerical Simulation of Properties of a LPG Flame with High-Temperature Air* 10International Journal of Thermal Sciences
35. *Design Optimization of Flameless-oxyfuel Soaking Pit Furnace Using CFD Technique* Energy Procedia
36. *Analysis of the experimental data collected during the OXYFLAME-3 Staged and Premixed Flames* IFRF DOCD 85/y/5
37. *Emission control of nitrogen oxides in the oxy-fuel process* 5Progress in Energy and Combustion Science
38. *Oxy-fuel combustion of solid fuels* 5Progress in Energy and Combustion Science
39. *New Weighted Sum of Gray Gases Model Applicable to Computational Fluid Dynamics (CFD) Modeling of Oxy−Fuel Combustion: Derivation, Validation, and Implementation* 12energy and fuels
40. *Accuracy evaluation of the gray gas radiation model in CFD simulation* Case Studies in Thermal Engineering
41. *Evaluation of solution methods for radiative heat transfer in gaseous oxy-fuel combustion environments* 14Journal of Quantitative Spectroscopy and Radiative Transfer
42. *Numerical Simulation of Combustion Characteristics in High Temperature Air Combustion Furnace* 2Journal of Iron and Steel Research, International
43. *Application of oxyfuel combustion in reheating at Ovako,Hofors works, Sweden – Background, solutions and results*Linde AGA2006
44. *Flameless oxyfuel combustion: technology,* La Revue de Métallurgie-CIT2006
45. *Oxygen-Enhanced Combustion, Second Edition*2013ISBN 9781439862285 - CAT# K12887
46. *Experimental and Numerical Study of Flameless Combustion in a Model Gas Turbine Combustor* 2Combustion Science and Technology
47. *Flameless oxidation to reduce thermal NO-formation* Prog. Energy Combust. Sci
48. *What is Flameless Combustion?*IFRF Online Combustion Handbook2002ISSN 1607-9116